Applied Microbiology and Biotechnology
https://doi.org/10.1007/s00253-018-9056-8

APPLIED GENETICS AND MOLECULAR BIOTECHNOLOGY

A novel signal transduction system for development of uric acid biosensors

Yongpeng Yao [1,2] · Shanshan Li [1,3] · Jiaqian Cao [1,2] · Weiwei Liu [1,2] · Fengxian Qi [1,2] · Wensheng Xiang [3] · Keqian Yang [1] · Weishan Wang [1] · Lixin Zhang [1,4,5,6]

Received: 12 February 2018 / Revised: 24 April 2018 / Accepted: 27 April 2018
© Springer-Verlag GmbH Germany, part of Springer Nature 2018

Abstract

Uric acid (UA) is an important biomarker for clinical diagnosis. Here, we present a novel signal transduction system for the development of UA biosensors with the characteristics of stability and ease-of-use. In this system, bacterial allosteric transcription factor HucR was used as the bio-recognition element, and the competition between HucR and the restriction endonuclease *Hin*dIII-HF to bind to the designed DNA template was employed to enable signal transduction of UA recognized by HucR. The presence of UA can induce conformational change of HucR, which dissociates HucR from the designed DNA template, allowing the access of the competitor *Hin*dIII-HF to cut this DNA template. Thus, the signal of UA recognized by HucR is transduced to easily detectable DNA signal. As proof-of-concept, we demonstrated two UA biosensors by coupling this signal transduction system with real-time quantitative PCR (RT-qPCR) and amplified luminescent proximity homogeneous assay (Alpha), respectively. The RT-qPCR-based UA biosensor has a detection limit of 5 nM with a linear range up to 300 nM UA; Alpha-based UA biosensor has a detection limit of 30 nM with a linear range of 100 nM–10 μM. Moreover, the robustness of both biosensors was verified by reliably detecting UA present in a human serum sample. Altogether, the novel UA biosensors developed in this work hold great potential for clinical application.

Keywords Signal transduction system · Allosteric transcription factor · Restriction enzyme · Uric acid biosensor

Introduction

Uric acid (UA) is a primary metabolic product of purine and its derivatives in human. It is a key biomarker for the diagnosis of several diseases, for instance, gout, Lesch–Nyhan syndrome, hyperuricemia, and leukemia (Perez-Ruiz et al. 2015; Zuo et al. 2011). The development of ease-of-use UA biosensors is therefore of great importance for the early stage warning of these diseases. Current available UA biosensors take uricase and its catalyzing UA oxidation reaction as the

Yongpeng Yao and Shanshan Li contributed equally to this work.

Electronic supplementary material The online version of this article (https://doi.org/10.1007/s00253-018-9056-8) contains supplementary material, which is available to authorized users.

✉ Keqian Yang
yangkq@im.ac.cn

✉ Weishan Wang
wangws@im.ac.cn

✉ Lixin Zhang
zhanglixin@im.ac.cn

[1] State Key Laboratory of Microbial Resources and CAS Key Laboratory of Pathogenic Microbiology and Immunology, Institute of Microbiology, Chinese Academy of Sciences, Beijing 100101, People's Republic of China

[2] University of Chinese Academy of Sciences, Beijing 100049, People's Republic of China

[3] State Key Laboratory for Biology of Plant Diseases and Insect Pests, Institute of Plant Protection, Chinese Academy of Agricultural Sciences, Beijing 100193, People's Republic of China

[4] State Key Laboratory of Bioreactor Engineering, East China University of Science and Technology, Shanghai 200237, People's Republic of China

[5] Laboratory for Marine Biology and Biotechnology, Qingdao National Laboratory for Marine Science and Technology, Qingdao 266061, People's Republic of China

[6] Key Laboratory for Biosensor of Shandong Province, Biology Institute, Shandong Academy of Sciences, Jinan 250014, People's Republic of China

Published online: 30 June 2018

signal recognition and signal transduction, respectively. Then, the H_2O_2 generated by enzymic oxidization of UA is further coupled with various signal amplification technologies, including gold nanoclusters (Liu et al. 2017), semiconductor nanoparticles (Jin et al. 2016; Jindal et al. 2013), quantum dots (Azmi et al. 2015), and so on. These biosensors may suffer from similar issues in practical application, e.g., poor aqueous solubility, and vulnerability to the more complex matrix. Given that the accurate detection of UA is required for both clinical monitoring and diagnosis (Rock et al. 2013), there is an urgent need for robust and convenient alternative UA biosensors with quite different working principle. Therefore, the development of novel signal transduction system coupling with new types of bio-recognition elements of UA will have the genuine contributions to UA detection.

Deinococcus radiodurans can respond to UA by a MarR family allosteric transcription factor HucR (Wilkinson and Grove 2004). HucR represses the transcription of *dr1160* which encodes a hypothetical uricase, and this repression can be relieved by the efficient antagonist UA (Wilkinson and Grove 2004; Wilkinson and Grove 2005). The ability of specific response to UA enables HucR being an ideal bio-recognition element for the development of novel UA biosensors (Li et al. 2016). To get novel UA biosensors, the challenge now is how to efficiently and faithfully transduce the signal of UA recognized by HucR to easily detectable signals. Only a signal transduction system with characteristic of ease-of-use and stability can meet the requirements of UA detection and advance its application in clinical diagnosis.

An ideal signal transduction system could transduce the UA signal sensed by HucR to an easily detectable signal. Considering that a variety of mature and robust DNA detection methods are used ubiquitously throughout life science and clinical medicine, such as the commercialized real-time quantitative PCR (RT-qPCR) (Kubista et al. 2006), digital PCR (Morley 2014), loop-mediated isothermal amplification (LAMP) (Zhang et al. 2014), recombinase polymerase amplification (RPA) (Zhao et al. 2015), aggregation of gold nanoparticles (AuNPs) (Saha et al. 2012), and molecular beacon (MB) (Zheng et al. 2015), thus, we concentrated on how to transduce the UA recognition of HucR to the easily detectable DNA signal in the current work.

In *D. radiodurans*, the regulatory role of HucR is achieved by the competition against RNA polymerase to bind to the target promoter region (Wilkinson and Grove 2004). Inspired by this natural scenario, we proposed that HucR could compete against other DNA-binding proteins to bind to the designed DNA sequences containing the binding site of HucR (*hucO*) in vitro. In this work, we chose type II restriction endonuclease (RE) (Pingoud et al. 2014) *Hin*dIII-HF as the competitor, which reliably targets the recognition site to cut the DNA sequence. Thereby, the signal transduction from UA (target small molecule) to easily detectable DNA could be implemented by employing the competition between HucR and *Hin*dIII-HF to bind to the designed DNA template. Further, we selected the widely used RT-qPCR (Kubista et al. 2006) and amplified luminescent proximity homogeneous assay (Alpha) (Burlein et al. 2014; Ullman et al. 1994) as examples to couple this novel signal transduction system and demonstrated the construction of two robust and ease-of-use UA biosensors. The satisfied performance of these biosensors highlights their promise as alternative approaches for UA detection in clinic diagnosis.

Materials and methods

Reagents

The oligonucleotides (Table S1) used in this work were synthesized and purified by Sangon Biotech Co. Ltd. (Beijing, China). *Hin*dIII-HF was purchased from New England Biolabs (Beijing, China). 2 × FastFire RT-qPCR PreMix was obtained from Tiangen Biotech Co. Ltd. (Beijing, China). Human serum samples were purchased from Beijing Solarbio Science & Technology Co., Ltd. All of the solutions were prepared in sterilized Milli-Q water (MQ, purified by Millipore). All other chemical reagents used in this work were analytical grade without further purification.

Plasmid construction

The optimized coding sequence (Table S2) of *hucR* gene (GeneBank Accession number MH001520) was synthesized by Synbio-Tech (Suzhou, China). Then, the sequence of HucR was cloned into the *Nde*I and *Xho*I restriction sites of pET23b (Novagen), resulting in the recombinant HucR with C-terminal His-tag. The construction was confirmed by sequencing.

Expression and purification of HucR

The recombinant HucR was expressed in *Escherichia coli* BL21 (DE3). Purification of HucR was performed as previously described (Wang et al. 2016c). The concentration of purified HucR was determined by the Bradford method using bovine serum albumin (BSA) as a standard. The purified HucR were analyzed by 18% sodium dodecyl sulfate polyacrylamide gel electrophoresis (SDS-PAGE).

Bio-layer interferometry assay

Kinetics between HucR and its target-binding site (DNA_{TFBS}) were determined by bio-layer interferometry (BLI) assay using an Octet RED96 system (FortéBIO) as previously described (Li et al. 2016). Briefly, the process consisted of five

steps: balance, DNA loading, rebalance, association, and dissociation. The blank tests were carried out using HBS-EP buffer (Li et al. 2016) instead of HucR in the association step and were used for baseline correction.

Verification of the competition of HucR and *Hin*dIII-HF on DNA_{TFBS}

The competitive interaction between HucR and *Hin*dIII-HF on the designed DNA sequence (Table S1) was demonstrated by native PAGE. T_{L+R}, T_L, and T_R were obtained by annealed primers (T_{L+R}-s and T_{L+R}-as for T_{L+R}, T_L-s and T_L-as for T_L, T_R-s and T_R-as for T_R, Table S1). Then, different concentrations of HucR (0, 0.17, 1.7, 3.4, 16.8, and 33.5 μM), 200 nM T_{L+R}, and 1 × CutSmart buffer (50 mM potassium acetate, 20 mM Tris-acetate, 10 mM magnesium acetate, 100 μg/mL BSA, pH 7.9) in a volume of 20 μL were incubated at 25 °C for 20 min to allow complete interaction between protein and DNA. After that, 3 U *Hin*dIII-HF was added and further incubated at 37 °C for 15 min. The reaction was terminated by heating the mixture at 85 °C for 20 min and slowly cooling to room temperature. Next, the complexes were mixed with 5 × loading buffer (100 mM Tris, 25% (*v*/*v*) glycerol, 0.2 mg/mL BSA, pH 7.9) and loaded onto a native gel. The native gel (15% polyacrylamide) was prepared by adding 5 mL 30% acrylamide (acrylamide:bis-acrylamide (m/m), 29:1), 1 mL 10 × TBE buffer (890 mM Tris, 890 mM boric acid, and 20 mM EDTA, pH 8.0), 5 μL TEMED, and 50 μL 10% ammonium persulfate to a total volume of 10 mL. Electrophoresis was performed at room temperature with 0.5 × TBE buffer (44.5 mM Tris-base, 44.5 mM boric acid, 0.05 mM EDTA, pH 8.0) as a running buffer. After electrophoresis, the gels were stained with SYBR Gold Nucleic Acid Gel Stain (Invitrogen) in 0.5 × TBE buffer for 30 min and photographed under an ultraviolet trans-illuminator (Bio-Rad GelDoc XR).

To test that whether UA could modulate the competition between HucR and *Hin*dIII-HF, the interaction among T_{L+R}, HucR, UA, and *Hin*dIII-HF was examined by native PAGE. UA with different concentrations (0, 0.01, 0.1, 0.5, 1, and 5 mM), 200 nM T_{L+R}, and 33.5 μM HucR to a total volume of 20 μL and the mixture were incubated at 25 °C for 20 min to allow the complete interaction between DNA, HucR, and UA. After that, 3 U *Hin*dIII-HF was added to the complexes and further incubated for 15 min at 37 °C. Finally, the reaction was terminated and detected by the 15% native PAGE as described above.

Optimizing the concentrations of components for UA biosensor coupling RT-qPCR

To optimize the template concentration for UA biosensor coupling with RT-qPCR output, the annealed template consisting of equal proportions of Template-s and Template-as (Table S1) was diluted from 20 f. to 20 nM, i.e., seven orders of magnitude. The volume of RT-qPCR was 20 μL, including 10 μL 2 × FastFire RT-qPCR PreMix, 2 μL annealed template, and 0.2 μM forward (F1, Table S1) and reverse (R1, Table S1) primers. The RT-qPCR reaction was performed on the Roche LightCycler® 480II real-time PCR system using hot start of 95 °C for 1 min, followed by 40 cycles at 95 °C for 5 s, 55 °C for 10 s, and 72 °C for 15 s. The real-time fluorescence intensity was simultaneously monitored after elongation of each cycle. The concentration of template used to construct the biosensor was optimized to a satisfied ratio of signal-to-noise (S/N > 3). S/N was calculated as $\Delta C_t/(\Delta C_{tmin})$. ΔC_t indicated the difference between cycle threshold (Ct) values of non-template control (NTC) and Ct values of samples. ΔC_{tmin} indicated the minimum ΔC_t. To optimize the concentration of HucR, the mixture (10 μL) containing 200 pM templates, HucR (ranging from 0.05 to 1.5 nM), and 1 × CutSmart buffer was incubated at 25 °C for 20 min to allow the binding of HucR on the annealed template. Then, 0.05 U *Hin*dIII-HF was added, and the mixture was incubated at 37 °C for 15 min for digestion. The digestion reaction was inactivated at 85 °C for 10 min. Then, RT-qPCR was conducted following the conditions mentioned above. The proper concentration of HucR was determined as the minimal amount of HucR that could completely inhibit *Hin*dIII-HF to cut the designed DNA.

To characterize the UA biosensor coupling with RT-qPCR output, 10 μL reaction mixture consisting of 200 pM annealed templates, 1 nM HucR, different amounts of UA from 0 to 300 nM, and 1 × CutSmart buffer were incubated at 25 °C for 20 min. The digestion and RT-qPCR reaction were implemented under the same conditions mentioned above. The limit of detection (LOD) was calculated based on 3σ/slope rule, where σ is the standard deviation of three blank samples (Xiang and Lu 2011).

Optimizing the concentrations of components for UA biosensor coupling Alpha

The modified linker DNA was obtained by annealing primers (L-HucR-s and L-HucR-as, Table S1). To optimize the concentration of linker DNA, the experiments were performed in 384-well white OptiPlates (PerkinElmer; No. 6007299) at room temperature. The reaction mixture (25 μL) contained 5 μL of modified linker DNA with a final concentration ranging from 1 pM to 10 nM, as well as an equal volume (5 μL) of donor beads and acceptor beads, with a final concentration of 20 μg/mL, and 10 μL of 1 × AlphaLISA universal assay buffer. The mixture was incubated in the dark for 60 min at room temperature. The luminescence signal was detected on an EnSpire Multimode Plate Reader (PerkinElmer). Raw data were processed by subtracting the luminescence signal of

the blank (substitute the modified linker DNA with the same volume of 1 × AlphaLISA universal assay buffer). The minimal concentration of linker DNA that generated a sufficient resolution (S/N > 10) was chosen to ensure high sensitivity of the UA biosensor. Then, the proper concentration of HucR was further optimized. First, 5 μL of modified linker DNA with a final concentration of 0.1 nM and 5 μL of HucR (with a final concentration ranging from 0.1 pM to 10 nM) was incubated together at 25 °C for 20 min. Then, 5 μL of 0.05 U *Hin*dIII-HF was added to the mixture. The digestion was incubated at 37 °C for 15 min and terminated by incubation at 85 °C for 10 min. After slowly cooling to room temperature, 5-μL aliquots of acceptor and donor beads were sequentially added to the mixture to a final concentration of 20 μg/mL. The mixture was incubated in the dark for 60 min, and the luminescence signal was measured as described above. When the luminescence increased to a relatively constant level, the lowest concentration of HucR was chosen as the optimal.

To characterize the UA biosensor coupling with luminescence output, equal volume (5 μL) of 1 nM HucR and 0.1 nM modified linker DNA and different concentrations of UA (ranging from 0.03 nM to 1 mM) were incubated together at 25 °C for 20 min. After that, 5 μL of 0.05 U *Hin*dIII-HF was added, and the mixture was continuously incubated at 37 °C for 15 min and further heated at 85 °C for 10 min to terminate the digestion. When the mixture slowly cooled to the room temperature, 5-μL aliquots of donor and acceptor beads were sequentially added to a final concentration of 20 μg/mL, and the mixture was incubated in the dark for 60 min for further luminescence detection. The LOD of the biosensor was determined as the minimal concentration of UA that gave a detectable signal change compared to the blank control.

Results

Principle of the signal transduction system

The detailed principle of this novel signal transduction system is illustrated in Fig. 1. The DNA template contains a *Hin*dIII-HF recognition site close to *hucO*. When UA is absent, the HucR binds to *hucO* and blocks the interaction between *Hin*dIII-HF and this template by steric hindrance. In contrast, the presence of small molecule analyte promotes the dissociation of HucR from *hucO*, allowing *Hin*dIII-HF to bind to its recognition site and cut the DNA template into two parts. By this way, the UA signal perceived by HucR is transduced to an easy-to-detect DNA signal (the "split" DNA template). The intact or "split" DNA template can be conveniently detected by many mature and robust DNA detection methods, including RT-qPCR (Kubista et al. 2006), digital PCR (Morley 2014), LAMP (Zhang et al. 2014), RPA (Zhao et al. 2015), AuNPs (Saha et al. 2012), MB (Zheng et al. 2015),

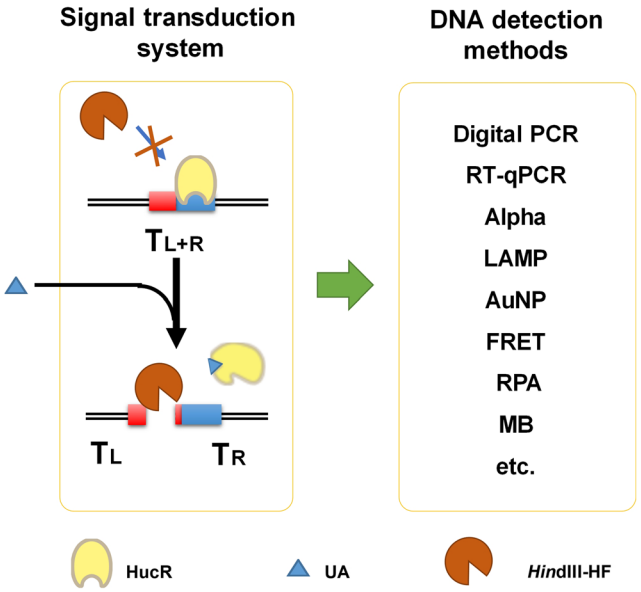

Fig. 1 Principle of the signal transduction system. The *hucO* and RE recognition site are indicated with a blue and red rectangle, respectively. RT-qPCR, real-time quantitative PCR; Alpha, amplified luminescent proximity homogeneous assay; LAMP, loop-mediated isothermal amplification; AuNPs, aggregation of gold nanoparticles; FRET, fluorescence resonance energy transfer; RPA, recombinase polymerase amplification; MB, molecular beacon

fluorescence resonance energy transfer (FRET) (Howell 2006), and so on.

Verification of the signal transduction system

The recombinant HucR was firstly expressed and purified to homogeneity (Fig. 2a). Then, BLI assay was used to test the activity of purified HucR, and the results confirmed the specific interaction between HucR and the DNA sequence containing *hucO*, as well as UA-triggered dissociation of HucR from HucR-DNA complexes (Fig. 2b). Subsequently, the competitive binding of HucR and *Hin*dIII-HF on the designed DNA template was tested by native PAGE. As shown in Fig. 2c, *Hin*dIII-HF cut the DNA template into two parts, but such a cutting reaction was inhibited by HucR in a concentration-dependent manner, indicating the competition of HucR and *Hin*dIII-HF indeed occurred on the designed DNA template. Further, whether the addition of UA could "rescue" the cutting reaction was also tested, and we observed that the amount of cut DNA products increased in a UA concentration-dependent manner (Fig. 2d). These results strongly support that our proposed signal transduction system can transduce the signal perceived by the HucR to DNA signal (i.e., the "split" DNA template). As proof-of-concept, we further used this signal transduction system to couple the UA recognition of HucR with two DNA detection methods: RT-qPCR (Kubista et al. 2006) and Alpha (Burlein et al. 2014; Ullman et al. 1994).

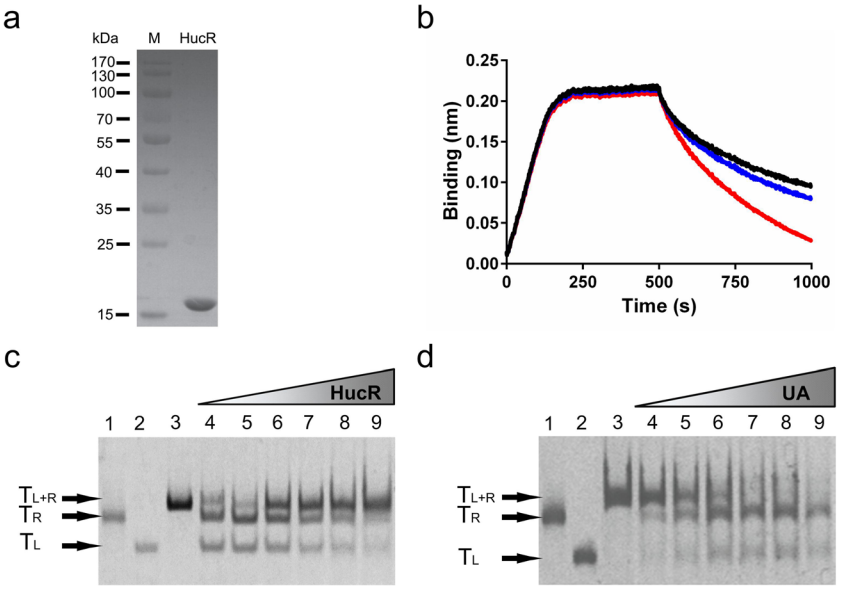

Fig. 2 Verification of the signal transduction system. **a** Purification of recombinant HucR. Recombinant HucR was examined by SDS-PAGE. Lane M, protein marker (15–170 kD). **b** Sensogram of interaction between HucR and DNA sequence containing *hucO* with or without UA by BLI. Bio-DNA containing *hucO* (10 ng/μL) was loaded on the streptavidin sensor and then interacted with 1.0 nM HucR (black line), 20 nM HucR and 1 nM UA (blue line), and 20 nM HucR and 10 nM UA (red line). **c** Demonstration of the competition between *Hin*dIII-HF and HucR on the linker DNA (T_{L+R}) by electrophoresis. Lane 1, digested product (T_R) of T_{L+R}. Lane 2, digested product (T_L) of T_{L+R}. Lane 3, T_{L+R}. Lanes 4 to 9, the concentrations of HucR were 0, 0.17, 1.7, 3.4, 16.8, and 33.5 μM, respectively, and the concentration of *Hin*dIII-HF was 0.15 U/μL for each of them. **d** Modulation of the competition between HucR and *Hin*dIII-HF by UA. Lane 1, T_R. Lane 2, T_L. Lane 3, T_{L+R}. Lanes 4 to 9, the concentrations of *Hin*dIII-HF and HucR in each lane were 0.15 U/μL and 33.5 μM, respectively. The concentrations of UA were 0, 0.01, 0.1, 0.5, 1, and 5 mM, respectively

Development of a UA biosensor by coupling the signal transduction system with RT-qPCR

Using this signal transduction system, a novel UA biosensor was implemented by coupling the recognition of HucR with RT-qPCR. The principle is illustrated in Fig. 3a, and the designed DNA template harboring both the *Hin*dIII-HF recognition site and HucR binding site *hucO* is shown in Fig. 3b. When the UA is absent, the HucR binds to the *hucO* and blocks the interaction between *Hin*dIII-HF and the template. Thus, the cutting of the template by *Hin*dIII-HF is repressed, and the intact template can be then amplified by RT-qPCR. In the presence of UA, the HucR is released from the template, allowing *Hin*dIII-HF to work on its recognition and cutting site. Thus, the amount of intact template is decreasing and causing an increase of Ct values outputted by RT-qPCR.

To get a satisfied signal, the appropriate concentration of DNA template was determined according to the template dependent fluorescence-time curves (Fig. S1a). Here, 200 pM of DNA templates could provide a satisfied output signal resolution (S/N > 3) (Fig. S1b). Then, the concentration of HucR was optimized. The Ct value of RT-qPCR showed negative correlation with the concentration of HucR (Fig. S2a), indicating that the competition between HucR and *Hin*dIII-HF to bind to the designed template could be outputted by RT-qPCR. As 1 nM of HucR could reduce the Ct value to nearly the same level of that of the non-template control (NTC) (Fig. S2b), this concentration was adopted to construct the UA biosensor. Under the optimal concentration of the template and HucR, this UA biosensor gave a panel of typical S-shaped fluorescence-PCR cycle number curves with different UA concentrations (Fig. 3c). According to the linear relationship between Ct value and the logarithm of UA concentration, UA can be accurately quantified within the range of 5–300 nM (Fig. 3d), and the LOD was calculated to be 1.06 nM based on 3σ/slope rule (Xiang and Lu 2011).

Development of a UA biosensor by coupling the signal transduction system with Alpha

In addition to RT-qPCR, we also developed another UA biosensor coupling our signal transduction system to Alpha with luminescence output. The principle is illustrated in Fig. 4a. The linker DNA contains a *Hin*dIII-HF recognition site close to *hucO*, and the 5′ ends of both strands are covalently modified by biotin and digoxin, respectively (Fig. 4b). Thus, streptavidin-coated donor beads and anti-digoxin antibody-coated acceptor beads are linked together by specific interactions with the modified linker DNA, and their distance is within the effective diffusion range of singlet state oxygen ($^1O_2$) (< 200 nm). When the small molecule analyte

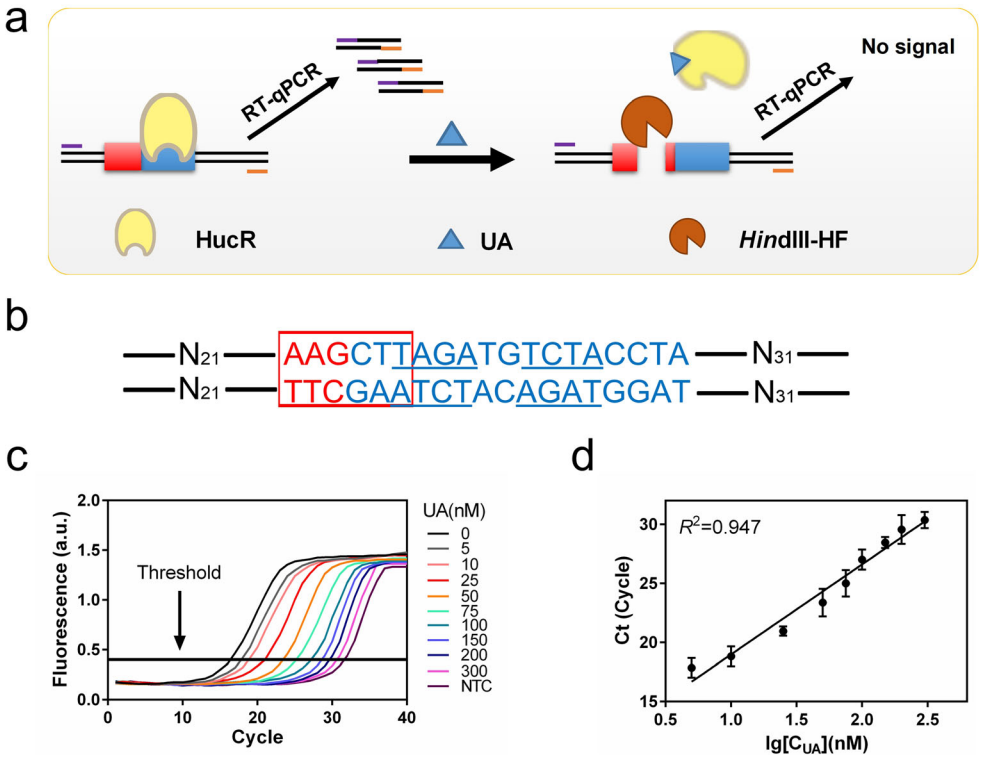

Fig. 3 UA biosensor by coupling the developed signal transduction system with RT-qPCR. **a** Working mechanism of the RT-qPCR-based UA biosensor. The *hucO* and *Hin*dIII-HF recognition sites are indicated with blue and red rectangles in the template DNA, respectively. **b** The sequence of template DNA. The *hucO* is indicated with blue base-pairs. The palindromic sequence in the *hucO* is underlined. The *Hin*dIII-HF recognition site is indicated in red box. The primers of RT-qPCR are designed at the end of linker DNA. **c** Amplification plot of RT-qPCR with different UA concentrations in the range of 0–300 nM. NTC was the non-template control. **d** Relationship between Ct value and UA concentration. Experiments were performed in triplicate. Data were the average of three repeats. For **d**, results were expressed as mean ± standard deviation (SD)

is absent, the HucR binds to its *hucO* and blocks the interaction between *Hin*dIII-HF and linker DNA. Upon laser excitation at 680 nm, the photosensitizer inside the donor beads converts ambient oxygen to excited $^1O_2$, which can diffuse to the adjacent acceptor beads and make the acceptor beads produce extensive luminescence signals at 615 nm. In contrast, the presence of small molecule analyte promotes the dissociation of HucR from *hucO*, then *Hin*dIII-HF binds to its recognition site and cuts the linker DNA into two parts, causing the separation of donor beads from acceptor beads. Therefore, $^1O_2$ cannot diffuse to the acceptor beads to trigger luminescence.

To get a satisfactory luminescence signal (S/N > 10), the concentrations of linker DNA and HucR were optimized as 0.1 and 1.0 nM, respectively (Fig. S3a and b). Under the optimal conditions, performance of this biosensor was characterized. Luminescence signal showed a UA concentration-dependent manner (Fig. 4c, d): an obvious luminescence signal change was observed when the concentration of UA was higher than 30 nM; and the change of luminescence signal reached a plateau value when the UA concentration was more than 10 μM. Thus, UA can be detected in the range of 100 nM–10 μM, and the LOD was determined to be 30 nM.

Selectivity and reproducibility of the developed UA biosensors

Under the optimal conditions, the selectivity of the two UA biosensors was evaluated. Analogues of UA including xanthine, guanine, hypoxanthine, and adenine were measured by both UA biosensors. We observed that the analogues of UA could not be detected even at higher concentration using both of our developed UA biosensors (Fig. 5a, b). These results indicated the proposed strategy could detect UA with satisfactory sensitivity and selectivity. Reproducibility of the constructed UA biosensors was evaluated by relative standard deviation (RSDs) of six repetitive measurements for three different levels of UA. The RSDs of the UA biosensor with RT-qPCR output were 6.4, 7.1, and 5.7% for 10, 50, and 100 nM UA, respectively; and the RSDs of the UA biosensor with luminescence output were 9.4, 8.7, and 7.7% for 500 nM, 1 μM, and 10 μM UA, respectively. These results indicate the satisfactory reproducibility for UA detection.

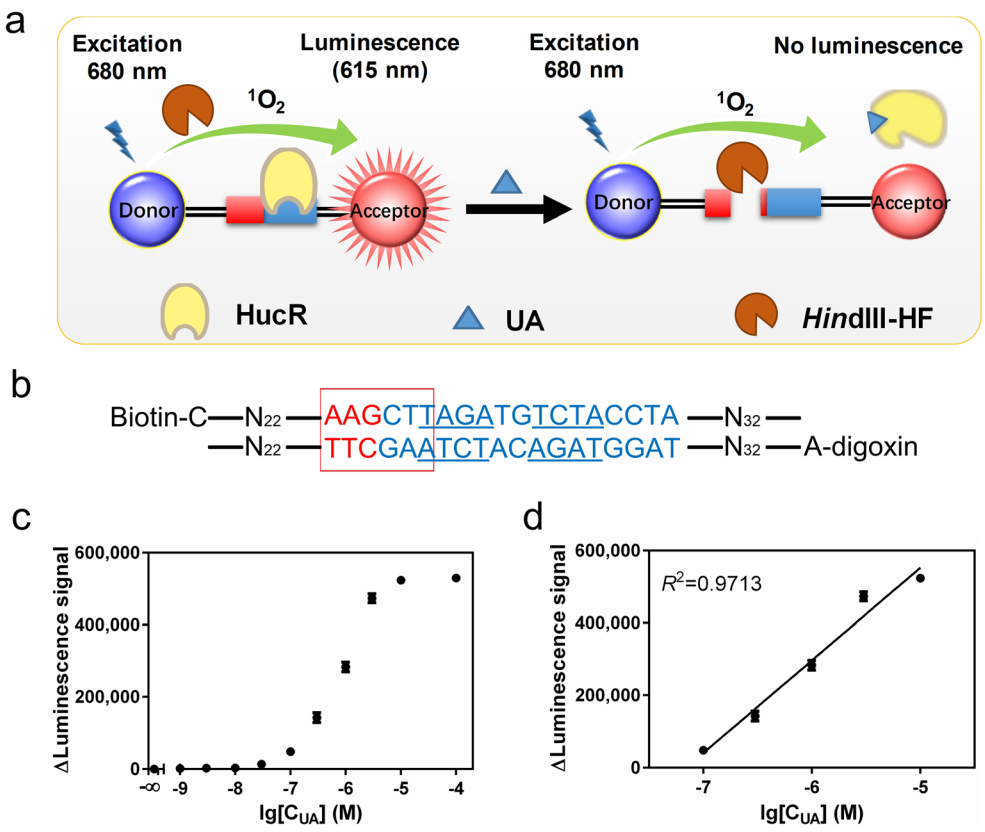

Fig. 4 UA biosensor by coupling the developed signal transduction system with Alpha. **a** Working mechanism of Alpha-based UA biosensor. The *hucO* and *Hin*dIII-HF recognition sites are indicated with blue and red rectangles in the linker DNA, respectively. **b** The sequence of linker DNA. The *hucO* is indicated with blue base-pairs. The palindromic sequence in the *hucO* is underlined. The *Hin*dIII-HF recognition site is indicated in red box. The 5′ ends of both strands are covalently modified by biotin and digoxin, respectively. **c** Relationship between luminescence output and UA concentrations in the range of 0–100 nM. ΔLuminescence signal = $I_0 - I$. I_0 and I are the luminescence intensities of the sensing system without and with UA, respectively. **d** Linear relationship between ΔLuminescence signal and UA concentration. Experiments were performed in triplicate. Data were the average of three repeats. For **c** and **d**, results were expressed as mean ±SD

Application in real sample detection

To investigate the validity of the developed UA biosensors to clinical samples, recovery testing was carried out by spiking UA solution into human serum (diluted with PBS buffer). The spiked samples with the concentration of 200 nM and 1 μM of target were measured; the recoveries were 95–104% for UA biosensor with RT-qPCR output, and 92–107% for UA biosensor with luminescence output, respectively. These data indicate that the developed UA biosensors could be used in practical applications.

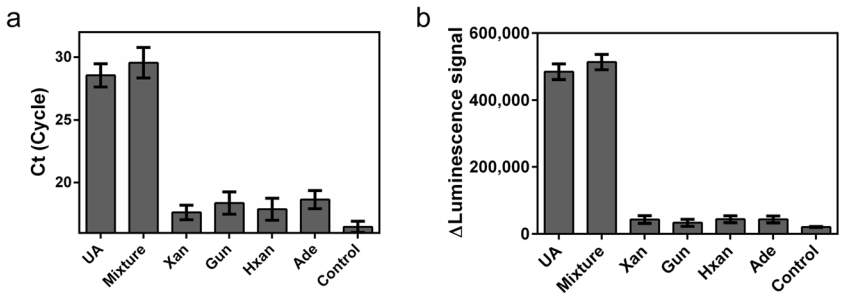

Fig. 5 Evaluation of the specificity of our developed biosensors. **a** Specificity of the RT-qPCR-based UA biosensor. For each chemical, 200 nM was used. Mixture contains 200 nM each chemicals of UA, Xan, Gua, Hxan, and Ade. **b** Specificity of the Alpha-based UA biosensor. For each chemical, 2 μM was used. Mixture contains 2 μM each chemicals of UA, Xan, Gua, Hxan, and Ade. UA, uric acid; Xan, xanthine; Gua, guanine; Hxan, hypoxanthine; Ade, adenine. Each reaction was run in triplicate, and data shown were the average of three repeats. Results were expressed as mean ± SD

Discussion

Development of UA biosensors is of great significance in clinic monitoring and diagnosis, as UA is an important biomarker of many diseases (Perez-Ruiz et al. 2015; Zuo et al. 2011). Current available UA biosensors usually use the uricase as the signal recognition element to catalyze the oxidization of UA to produce allantoin, CO_2, and H_2O_2, then H_2O_2 is further employed as transduction signal to trigger various reactions (Fang et al. 2016; Wang et al. 2016a; Wang et al. 2016b), such as coupling H_2O_2-sensitive quantum dots (Azmi et al. 2015). However, the instability of H_2O_2 gives these uricase-based biosensors some aspects of limitations such as poor sensitivity, stability, and reproducibility (Ghosh et al. 2015). In order to develop alternative UA biosensors with distinct principle, in this work, we designed and implemented a simple, efficient, and robust signal transduction system by employing a new type of UA signal recognition element HucR. Different to H_2O_2 produced by uricase, our signal transduction system can transduce the UA recognition of HucR to the DNA signal which is quite stable and easily quantified using various mature DNA detection methods. As proof-of-concept, coupling this system with RT-qPCR and Alpha, we have demonstrated two novel UA biosensors with high sensitivity (nanomolar levels, Figs. 3c and 4c), good selectivity (Fig. 5), and excellent reproducibility (RSDs < 10%). Compared with reported uricase-based UA biosensors, our aTF-based UA biosensor is one of the most sensitive ever reported, especially for UA biosensor coupling with RT-qPCR output (Table S3). In addition to the sensitivity, the significant advantage of our UA biosensor is that UA could be detected in an easy-to-implement manner with two modes of signal output (RT-qPCR mode and luminescence mode). These results demonstrate that our signal transduction system is reliable, robust, and ease-of-use and could fulfill the requirements of clinical diagnosis.

Our UA signal transduction system transduces the UA recognition of HucR to "split" DNA signal, which is compatible to many reliable and cost-effective DNA detection methods in theory. In addition to RT-qPCR and Alpha used in this work, there are various mature DNA detection methods and kits which are commercially available for laboratory test or on-site detection, such as digital PCR (Morley 2014), LAMP (Zhang et al. 2014), RPA (Zhao et al. 2015), and AuNPs (Saha et al. 2012). Therefore, coupling our signal transduction system with these different DNA detection methods, diverse UA biosensors can be constructed with various detection sensitivity and linear range to meet the different UA detection requirements.

In summary, we demonstrate a new signal transduction system for the development of UA biosensors with improved features. This system could transduce the signal of UA recognized by HucR to easily detectable DNA signal. Thus, the mature and robust DNA detection methods could be extended to the quantification of UA. As proof-of-concept, two novel UA biosensors were developed by coupling with the widely used RT-qPCR and Alpha. The sensitivity, stability, and ease-of-use characteristics of the UA biosensors highlight its potential as an alternative approach for UA detection in clinic diagnosis. Overall, this work provides a new strategy for the development of UA biosensors. Considering that large numbers of aTFs in bacteria show high specificity to diverse small molecule effectors (Libis et al. 2016), our work has reference significance to develop other aTF-based small molecule biosensors.

Acknowledgments We dedicate this paper to and in memory of our beloved friend, supervisor and colleague, Prof. Keqian Yang, who devoted his life to *Streptomyces* physiology, antibiotic biosynthesis, and molecular regulation.

Funding information This work was supported by grants from the National Natural Science Foundation of China (31320103911, 31430002, 31770055, 31570031, and 31772242), the Youth Innovation Promotion Association of CAS (2016087), the International Partnership Program of Chinses Academy of Science (153211KYSB20170014), and the Fundamental Research Funds for the Central Universities (22221818014).

Compliance with ethical standards

Ethical statement This study does not contain any studies with human participants or animals performed by any of the authors.

Conflict of interest The authors declare that they have no conflict of interest.

References

Azmi NE, Ramli NI, Abdullah J, Abdul Hamid MA, Sidek H, Abd Rahman S, Ariffin N, Yusof NA (2015) A simple and sensitive fluorescence based biosensor for the determination of uric acid using H_2O_2-sensitive quantum dots/dual enzymes. Biosens Bioelectron 67:129–133. https://doi.org/10.1016/j.bios.2014.07.056

Burlein C, Bahnck C, Bhatt T, Murphy D, Lemaire P, Carroll S, Miller MD, Lai MT (2014) Development of a sensitive amplified luminescent proximity homogeneous assay to monitor the interactions between pTEFb and Tat. Anal Biochem 465:164–171. https://doi.org/10.1016/j.ab.2014.08.007

Fang A, Wu Q, Lu Q, Chen H, Li H, Liu M, Zhang Y, Yao S (2016) Upconversion ratiometric fluorescence and colorimetric dual-readout assay for uric acid. Biosens Bioelectron 86:664–670. https://doi.org/10.1016/j.bios.2016.07.055

Ghosh T, Sarkar P, Turner APF (2015) A novel third generation uric acid biosensor using uricase electro-activated with ferrocene on a Nafion coated glassy carbon electrode. Bioelectrochemistry 102:1–9. https://doi.org/10.1016/j.bioelechem.2014.11.001

Howell WM (2006) Detection of DNA hybridization using induced fluorescence resonance energy transfer. Methods Mol Biol 335:33–41. https://doi.org/10.1385/1-59745-069-3:33

Jin D, Seo M-H, Huy BT, Pham Q-T, Conte ML, Thangadurai D, Lee Y-I (2016) Quantitative determination of uric acid using CdTe

nanoparticles as fluorescence probes. Biosens Bioelectron 77:359–365. https://doi.org/10.1016/j.bios.2015.09.057

Jindal K, Tomar M, Gupta V (2013) Nitrogen-doped zinc oxide thin films biosensor for determination of uric acid. Analyst 138(15):4353–4362. https://doi.org/10.1039/c3an36695b

Kubista M, Andrade JM, Bengtsson M, Forootan A, Jonak J, Lind K, Sindelka R, Sjoback R, Sjogreen B, Strombom L, Stahlberg A, Zoric N (2006) The real-time polymerase chain reaction. Mol Asp Med 27(2–3):95–125. https://doi.org/10.1016/j.mam.2005.12.007

Li S, Zhou L, Yao Y, Fan K, Li Z, Zhang L, Wang W, Yang K (2016) A platform for the development of novel biosensors by configuring allosteric transcription factor recognition with amplified luminescent proximity homogeneous assays. Chem Commun (Camb) 53(1):99–102. https://doi.org/10.1039/c6cc07244e

Libis V, Delepine B, Faulon JL (2016) Sensing new chemicals with bacterial transcription factors. Curr Opin Microbiol 33:105–112. https://doi.org/10.1016/j.mib.2016.07.006

Liu Y, Li H, Guo B, Wei L, Chen B, Zhang Y (2017) Gold nanoclusters as switch-off fluorescent probe for detection of uric acid based on the inner filter effect of hydrogen peroxide-mediated enlargement of gold nanoparticles. Biosens Bioelectron 91:734–740. https://doi.org/10.1016/j.bios.2017.01.020

Morley AA (2014) Digital PCR: a brief history. Biomol Detect Quantif 1(1):1–2. https://doi.org/10.1016/j.bdq.2014.06.001

Perez-Ruiz F, Dalbeth N, Bardin T (2015) A review of uric acid, crystal deposition disease, and gout. Adv Ther 32(1):31–41. https://doi.org/10.1007/s12325-014-0175-z

Pingoud A, Wilson GG, Wende W (2014) Type II restriction endonucleases—a historical perspective and more. Nucleic Acids Res 42(12):7489–7527. https://doi.org/10.1093/nar/gku447

Rock KL, Kataoka H, Lai JJ (2013) Uric acid as a danger signal in gout and its comorbidities. Nat Rev Rheumatol 9(1):13–23. https://doi.org/10.1038/nrrheum.2012.143

Saha K, Agasti SS, Kim C, Li X, Rotello VM (2012) Gold nanoparticles in chemical and biological sensing. Chem Rev 112(5):2739–2779. https://doi.org/10.1021/cr2001178

Ullman EF, Kirakossian H, Singh S, Wu ZP, Irvin BR, Pease JS, Switchenko AC, Irvine JD, Dafforn A, Skold CN, Wagner DB (1994) Luminescent oxygen channeling immunoassay: measurement of particle binding kinetics by chemiluminescence. Proc Natl Acad Sci U S A 91(12):5426–5430. https://doi.org/10.1073/pnas.91.12.5426

Wang H, Lu Q, Hou Y, Liu Y, Zhang Y (2016a) High fluorescence S, N co-doped carbon dots as an ultra-sensitive fluorescent probe for the determination of uric acid. Talanta 155:62–69. https://doi.org/10.1016/j.talanta.2016.04.020

Wang J, Chang Y, Wu WB, Zhang P, Lie SQ, Huang CZ (2016b) Label-free and selective sensing of uric acid with gold nanoclusters as optical probe. Talanta 152:314–320. https://doi.org/10.1016/j.talanta.2016.01.018

Wang W, Yang T, Li Y, Li S, Yin S, Styles K, Corre C, Yang K (2016c) Development of a synthetic oxytetracycline-inducible expression system for *Streptomycetes* using *de novo* characterized genetic parts. ACS Synth Biol 5(7):765–773. https://doi.org/10.1021/acssynbio.6b00087

Wilkinson SP, Grove A (2004) HucR, a novel uric acid-responsive member of the MarR family of transcriptional regulators from *Deinococcus radiodurans*. J Biol Chem 279(49):51442–51450. https://doi.org/10.1074/jbc.M405586200

Wilkinson SP, Grove A (2005) Negative cooperativity of uric acid binding to the transcriptional regulator HucR from *Deinococcus radiodurans*. J Mol Biol 350(4):617–630. https://doi.org/10.1016/j.jmb.2005.05.027

Xiang Y, Lu Y (2011) Using personal glucose meters and functional DNA sensors to quantify a variety of analytical targets. Nat Chem 3(9):697–703. https://doi.org/10.1038/nchem.1092

Zhang X, Lowe SB, Gooding JJ (2014) Brief review of monitoring methods for loop-mediated isothermal amplification (LAMP). Biosens Bioelectron 61:491–499. https://doi.org/10.1016/j.bios.2014.05.039

Zhao Y, Chen F, Li Q, Wang L, Fan C (2015) Isothermal amplification of nucleic acids. Chem Rev 115(22):12491–12545. https://doi.org/10.1021/acs.chemrev.5b00428

Zheng J, Yang R, Shi M, Wu C, Fang X, Li Y, Li J, Tan W (2015) Rationally designed molecular beacons for bioanalytical and biomedical applications. Chem Soc Rev 44(10):3036–3055. https://doi.org/10.1039/c5cs00020c

Zuo Y, Yang Y, Zhu Z, He W, Aydin Z (2011) Determination of uric acid and creatinine in human urine using hydrophilic interaction chromatography. Talanta 83(5):1707–1710. https://doi.org/10.1016/j.talanta.2010.11.073